Supplemental files

Supplemental Material and Methods

Synthesis of anti-CD37-ATACs

Cysteine reactive linker amanitin compounds with cleavable (Ama 1, Ama 2) or stable (Ama 3) linker were conjugated to engineered cysteine residues of an anti-CD37 antibody using maleimide chemistry. In brief, antibodies with engineered cysteines in PBS (pH 7.4) were reduced by Tris (2-carboxyethyl) phosphine and interchain cysteines were re-oxidized by dehydroascorbic acid. Subsequently, cysteine reactive linker amanitin compounds were conjugated to the engineered cysteines. All conjugates were purified by size exclusion-fast protein liquid chromatography. Drug-antibody ratio (DAR) was 2 toxins per IgG according to liquid chromatography-mass spectrometry analysis.

In vitro cytotoxicity assay

Cells were seeded and treated at a density of $2x10^4$ cells/mL in a 96-well plate and incubated for 96h. Cytotoxicity of anti-CD37-ATACs and α-amanitin was analyzed by using the cell viability assay CellTiter Glo 2.0 (Promega, Mannheim, Germany). Data analysis was performed with GraphPad Prism 7 (GraphPad Software, Inc. La Jolla, CA) software to plot curve fits and calculate half-maximal effective concentration (EC_{50}) values.

Cell lines

Raji ($CD37^{pos}$) and $HEK293^{wt}$ ($CD37^{neg}$) cell lines were obtained from German Collection of Microorganisms and Cell Cultures (DSMZ) and Cell Line services (CLS), respectively. $HEK^{OATP1B3}$ cell line was generated by HDPR.[1]

Determination of the Maximum Tolerated Dose and amanitin in vivo toxicity

All experiments were carried out following the guidelines of the German Animal Welfare Act and all relevant laws and regulations. Protocols were approved by the local regulatory authority

(Regierungspräsidium Karlsruhe, Germany, file number: G-64_21). The tolerability of compounds was tested in 6–8-week-old NOD/SCID/gamma chain$^{-/-}$ (NSG) female mice. The conjugates were diluted in PBS (pH 7.4). Survival and clinical signs were determined daily. The body weight was determined twice a week. Three animals per group were intravenously injected with increasing dose starting from a dose with no effect until termination criteria as defined in the animal protocol were met (e.g., net body weight loss of more than 20%, hypoactivity, paralysis, poor general health condition).

To determine amanitin hepatic toxicity, NSG mice were treated with vehicle o anti-CD37 Ama 1/Ama 2/Ama 3 at 5-10-40 mg/kg, respectively. Mice were euthanized 7 or 21 days after treatment. Blood and liver were collected. Serum was recovered to measure hepatic enzymes (ALT, AST and GGT) using the Catalyst One instrument (Idexx Laboratories, Hoofddorp, NL), while liver was formalin-fixed and paraffin embedded and H/E performed to check for signs of toxicity.

In vitro transcription RNA polymerase II inhibition assay

The inhibition of RNA polymerase II by the active metabolites of CD37-ATACs and α-amanitin was evaluated using the HeLaScribe Nuclear Extract in vitro Transcription System (Promega, Mannheim, Germany) and subsequent QuantiFast Probe RT-PCR Plus kit (Qiagen, Venlo, Netherlands). Data analysis was performed with GraphPad Prism 7 (GraphPad Software, Inc. La Jolla, CA) software to plot curve fits and calculate half-maximal inhibitory concentration (IC_{50}) values.

Expression of CD37 by quantitative reverse transcription polymerase chain reaction (qRT-PCR) and RNA sequencing data

RNA was extracted using RNeasy Plus Mini kit (Qiagen, Milan, Italy) and converted to cDNA using the High-Capacity cDNA Reverse Transcription kit (Applied Biosystems-Thermo Fisher Scientific, Milan, Italy). qRT-PCR was performed using the 7900 HT Fast Real Time PCR System (SDS 2.3 software). Primers for *CD37* (Hs01099648_m1) and *B2M* (Hs00984230_m1) were from Life

Technologies (Milan, Italy). Reactions were done in triplicate from the same cDNA reaction (technical replicates) and on samples derived from different RS cells obtained from RS-PDXs at different in vivo passages. For each gene, expression levels were computed as a ratio of the number of copies of the target gene over 10^5 copies of β2-microglobulin (*B2M*).

RS RNA was extracted from formalin-fixed paraffin-embedded (FFPE) section of RS primary sample biopsies, using the RNeasy FFPE kit (Qiagen) according to manufacturer's instructions. RNA sequencing was performed using the Stranded Total RNA Prep ligation with Ribo-Zero Plus kit (Illumina, Milan, Italy) on a NextSeq 550 platform (Illumina) and reads aligned using the DRAGEN RNA Pipeline (Illumina). Data on CD37 expression in B cell lines or primary samples corresponding to different hematological malignancies and different B cell differentiation stages were obtained from publicly available datasets, including TCGA, National Cancer Institute and European Genome-Phenome Archive. All used datasets are listed in Supplementary Table 1. ALL data from primary samples are based upon data generated by the Therapeutically Applicable Research to Generate Effective Treatments (https://ocg.cancer.gov/programs/target) initiative, phs000463. The data used for this analysis are available at https://portal.gdc.cancer.gov/projects.

Flow cytometry on CD37 expression and ATACs binding

CD37 expression on RS-PDXs was detected by an Alexa488-conjugated anti-CD37 antibody provided by Heidelberg Pharma. The binding capacity of the three anti-CD37 ATACs was analyzed in the four available RS-PDX models by flow cytometry. RS cells, freshly purified from tumor masses, were stained with the three anti-CD37 ATACs followed by an anti-human IgG-FITC-conjugated antibody (Agilent Dako, Carpinteria, CA). RS cells stained only with the anti-human FITC-conjugated antibody were used as negative control. Data were acquired using a FACS Celesta (BD Biosciences, Milan, Italy), processed with FlowJo v10.01 and binding evaluated as mean fluorescence intensity (MFI).

Expression of CD37 by western blot

Total lysates were resolved by SDS-PAGE gels and transferred to nitrocellulose membranes (BioRad, Milan, Italy). The expression of CD37 was confirmed by anti-CD37 antibody (Ab#251819 from Abcam, Milan, Italy). Bands were detected with an HRP-conjugated anti-rabbit antibody (sc-2004, Santa Cruz Biotechnology, Milan, Italy). An anti-actin HRP-conjugated antibody was used as a loading control (sc-1616, Santa Cruz Biotechnology). Blots were developed using enhanced chemiluminescence and images acquired with the ChemiDoc Imaging system (BioRad). Bands were quantified using the ImageLab software (BioRad).

Apoptosis assay

Freshly purified RS cells were cultured in a complete medium for 72 hours in the presence of different doses (40 and 200 nM) of anti-CD37 ATACs (anti-CD37-Ama 1, anti-CD37-Ama 2, anti-CD37-Ama 3). At the end of experiment, cells were collected, washed, and stained with AnnexinV APC-labelled/Propidium Iodide kit (Thermo Fisher Scientific) following manufacturer's instructions and samples analyzed by flow cytometry with a BD FACS Celesta.

In indicated experiments, peripheral blood mononuclear cells (PBMCs) from 6 healthy donors were cultured as indicated above, in the presence of irrelevant or anti-CD37 ATACs. Before AnnexinV/PI staining, B and T cells were stained with an anti-CD19-BV510 and CD3-BV650 antibodies, respectively (BD Biosciences).

Activation of the apoptotic pathway was confirmed by western blotting using anti-cleaved Caspase-3 (#9662) and anti-PARP (#9532) antibodies, all from Cell Signaling Technologies (Denvers, MA).

Immunohistochemistry (IHC) on RS-PDX models and primary RS samples

Formalin-fixed paraffin-embedded (FFPE) RS-PDX tumor sections as well as sections from primary RS biopsies and CLL-RS matched sample biopsies were stained with an anti-CD37 antibody (Ab#251819, Abcam), followed by an anti-rabbit HRP-conjugated antibody (Abcam) and 3,3'-diaminobenzidine (EnVision™ System, Dako) to visualize the reaction. Slides from RS-PDXs were

analyzed using an AXIO Lab.A1 microscope (Zeiss), equipped with a Canon EOS600D reflex camera and the images acquired using the ZoomBrowserEX software (Canon), while slides from primary samples were acquired with an Aperio Scan Scope scanner (Leica Biosystems, Milan, Italy). Anti-CD37 specificity on tissues was tested on reactive lymph nodes.

Patient-derived xenograft models of Richter's syndrome

Four different RS-PDX models were used in this study. All models, RS9737, RS1316, RS1050 and IP867/17 were established using the same experimental approach.[2] Genetic and phenotypic features of these models, reported in[3] are stable over-time and reflect the corresponding primary sample. Three of these models (RS9737, RS1316, and RS1050) were established from patients who had undergone extensive prior therapy and were resistant to conventional chemotherapy and/or targeted therapies (including R-CHOP and ibrutinib). In contrast, IP867/17 was established from a therapy-naive patient.

In vivo experiments

RS cells ($1x10^7$) were resuspended in PBS and injected into the tail vein of NSG mice. After 14 days of engraftment, mice were randomly assigned to treatment with vehicle (PBS), anti-CD37-Ama 2 (5 and 10 mg/kg), anti-CD37-Ama 3 (20 and 40 mg/kg) or anti-CD37-Ama 1 (2.5 and 5 mg/kg). ATACs were administered intravenously as a single treatment. After treatment administration, all mice were monitored for survival and euthanized when showing a clear disease-related morbidity (weight loss >20% or distress). At the time of euthanasia, peripheral blood (PB), kidneys, spleen, BM, lung, liver, and brain were collected to evaluate disease spread by flow cytometry, using anti-human antibodies (CD45PerCPCy5.5 and CD19APC, BD).

The Institutional Animal Care and Use Committee approved these experiments. Mice were treated following European guidelines for animal use in scientific research and with the approval of the Italian Ministry of Health (Authorization #664/2020-PR; protocol #CC652.136).

Statistical analysis

Statistical analyses were performed with GraphPad Prism v7. Differences were considered statistically significant when p-values were ≤0.05. The specific tests adopted to calculate the statistical significance are indicated in the figure legends.

References

1. Andreas Pahl CL, Torsten Hechler. Amatoxins as RNA Polymerase II Inhibiting Antibody–Drug Conjugate (ADC) Payloads. Cytotoxic Payloads for Antibody–Drug Conjugates: Royal Society of Chemistry; 2019:398-426.

2. Vaisitti T, Braggio E, Allan JN, Arruga F, Serra S, Zamo A, Tam W, Chadburn A, Furman RR, Deaglio S. Novel Richter Syndrome Xenograft Models to Study Genetic Architecture, Biology, and Therapy Responses. *Cancer Res*. 2018;78(13):3413-3420.

3. Vaisitti T, Arruga F, Vitale N, Lee TT, Ko M, Chadburn A, Braggio E, Di Napoli A, Iannello A, Allan JN, Miller LL, Lannutti BJ, Furman RR, Jessen KA, Deaglio S. ROR1 targeting with the antibody-drug conjugate VLS-101 is effective in Richter syndrome patient-derived xenograft mouse models. *Blood*. 2021;137(24):3365-3377.

Supplementary figures legend

Figure S1. Anti-CD37 ATAC structure and target-specific cytotoxicity. Schematic representation of amanitin conjugated to a chimeric anti-CD37 cysteine-engineered antibody with a cleavable linker at position L1 (CD37-Ama 1) or L2 (CD37-Ama 2) or with a non-cleavable linker at position L1 (CD37-Ama 3) **(A)**. Cytotoxicity of anti-CD37-ATACs (CD37-Ama 1: blue; CD37-Ama 2: green; CD37-Ama 3: red) on target-positive Raji cells **(B)** or target-negative HEK^{wt} cells **(C)**. Cytotoxicity of free α-amanitin on Raji (orange line), HEK^{wt} (black line) or $HEK^{OATP1B3}$ cells (grey line) **(D)**. Inhibition of RNA polymerase II by α-amanitin (black line) and active metabolite of CD37-Ama 2 (green line) **(E)**.

All experiments were done in triplicate and plotted as mean value and SEM.

Figure S2. CD37 is differentially expressed among B cell malignancies and present on primary RS samples and PDX models. CD37 expression was checked at the transcript level in several cell lines (**A**) or primary samples (**B**) corresponding to hematological malignancies derived from different B maturation stages. All data, except those referring to RS that were sequenced in the lab, were obtained from publicly available databases, and are expressed as Reads Per Kilobase Million (RPKM)**.** CD37 appeared to be expressed at low levels in early and late stages of differentiation, being present at high levels in mature B cells. CD37 expression on RS-PDX derived cells was confirmed also by flow cytometry analyses using an Alexa488 direct conjugated antibody (n=6/each model; **C**). The binding capacity of the three anti-CD37 ATACs (anti-CD37-Ama 1: blue; anti-CD37-Ama 2: green; anti-CD37-Ama 3: red) to RS cells was checked by flow cytometry, using an anti-human IgG FITC-conjugated antibody as a secondary reagent **(**n=6/each model; **D).**

ALL: acute lymphoblastic leukemia; CLL: chronic lymphocytic leukemia; MCL: mantle cell lymphoma; HL: Hodgkin's lymphoma; NHL: non-Hodgkin's lymphoma (includes Burkitt and diffuse large B cell lymphoma); MM: multiple myeloma; FL: follicular lymphoma; DLBCL: diffuse large B cell lymphoma; RS: Richter's syndrome; MFI: mean fluorescence intensity.

Figure S3. Anti-CD37 ATACs induce apoptosis in vitro. The apoptotic response of IP867/17 RS cells (n=5) exposed for 72 hours to different doses (40 and 200 nM) of anti-CD37-Ama 1, anti-CD37-Ama 2 and anti-CD37-Ama 3 ATACs or left untreated was analyzed with conventional cytofluorimetric AnnexinV/PI staining **(A).** Induction of apoptosis in RS-PDX-derived cells was confirmed by western blot analyses checking the activation and cleavage of PARP and Caspase-3 proteins. Actin was used as a loading control **(**n=3/each model; **B).** Protein bands referring to cleaved Caspase 3 and PARP following exposure of RS cells to anti-CD37 ATACs (72 hours) were quantified, normalized over actin and ratio of the cleaved band over the full-length one reported in the graphs.

Bas: basal condition; NT: vehicle-treated samples; FL: full-length; CL: cleaved.

Figure S4. Apoptotic response in normal B and T lymphocytes following anti-CD37 or irrelevant ADCs treatment. Peripheral blood mononuclear cells (PBMC) were incubated (72 hours) in the presence of 200 nM of non-targeting anti-Digitoxin or anti-CD37 antibodies conjugated to amanitin-derivatives Ama 1, Ama 2, Ama 3 with the same linkers. PBMCs were then stained with anti-CD19 or anti-CD3 antibodies before performing AnnexinV/PI staining. Viable cells are reported in the graphs. Asterisks over box plots refer to the statistical significance over the untreated condition (NT), while p values with bars refer to the indicated conditions.

Figure S5. Disease distribution in RS-PDX mice treated with anti-CD37 ATACs. Disease distribution in RS1316 **(A),** RS9737 **(B)** and RS1050 **(C)** PDX mice, euthanized because of the disease or because of the end of experiments. The main target organs were collected, dismantled and RS cells distribution analyzed by flow cytometry.

Kid: kidney; Liv: liver; BM: bone marrow; PB: peripheral blood; Bra: brain; Spl: spleen.

Figure S6. Evaluation of amanitin hepatic toxicity. H/E images (X200) of liver from mice treated with vehicle (PBS) or anti-CD37 Ama 1, Ama 2 and Ama 3 ADCs were obtained at 7 (A) and 21 days (B) after treatment. Picture from periportal and perivenular zones of the acinus were acquired with

a Leica DM 2000 LED microscope (Leica microsystem GmbH, Wetzlar, Germany). Acinar structure was preserved and no evidence of necrosis and inflammatory reaction was recognized. No differences were highlighted among the different groups of mice.

Supplementary Table 1. Sources of publicly available RNA sequencing datasets.

Type of data	Data source	Datasets
B cell lines	cBioPortal	https://www.cbioportal.org/study/summary?id=ccle_broad_2019
ALL primary samples	NIH Cancer Institute	https://ocg.cancer.gov/programs/target/data-matrix
CLL primary samples	European Genome-Phenome Archive	https://ega-archive.org/datasets/EGAD00001004046
FL primary samples	NIH Cancer Institute	https://ocg.cancer.gov/programs/cgci/data-matrix
DLBCL primary samples	NIH Cancer Institute	https://ocg.cancer.gov/programs/cgci/data-matrix
DLBCL primary samples	cBioPortal	https://www.cbioportal.org/study/summary?id=dlbc_tcga_pan_can_atlas_2018
Burkitt lymphoma primary samples	NIH Cancer Institute	https://ocg.cancer.gov/programs/cgci/data-matrix
MM primary samples	NCBI	https://www.ncbi.nlm.nih.gov/geo/query/acc.cgi?acc=GSE167968
ALL: acute lymphoblastic leukemia; CLL: chronic lymphocytic leukemia; FL: follicular lymphoma; DLBCL: diffuse large B cell lymphoma; MM: multiple myeloma.		

Supplementary Table 2. Liver enzymes values in vehicle- and ADC-treated mice.

Mouse ID	**ALT (U/L)**	**AST (U/L)**	**GGT (U/L)**
	7 days		
Vehicle	49	659.2	14
Anti-CD37 Ama1	619	1855	46
Anti-CD37 Ama2	121	1171.5	53
Anti-CD37 Ama3	746	2018	59
	21 days		
Vehicle	20	157	10
Anti-CD37 Ama1	312	1319	5
Anti-CD37 Ama2	42	472	9
Anti-CD37 Ama3	61	703	15
Range of values	**28-132**	**59-247**	

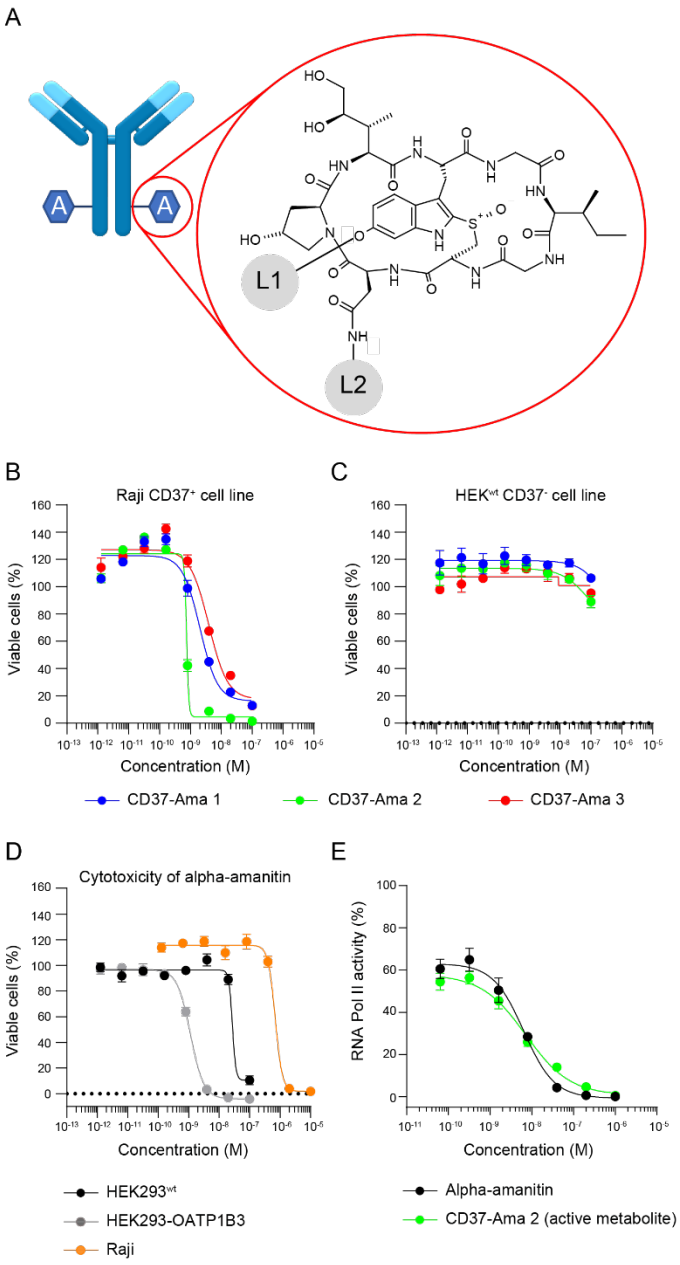
A
L1
L2
B
Raji CD37+ cell line
Viable cells (%)
Concentration (M)
C
HEKwt CD37- cell line
Viable cells (%)
Concentration (M)
CD37-Ama 1
CD37-Ama 2
CD37-Ama 3
D
Cytotoxicity of alpha-amanitin
Viable cells (%)
Concentration (M)
HEK293wt
HEK293-OATP1B3
Raji
E
RNA Pol II activity (%)
Concentration (M)
Alpha-amanitin
CD37-Ama 2 (active metabolite)

Figure S1

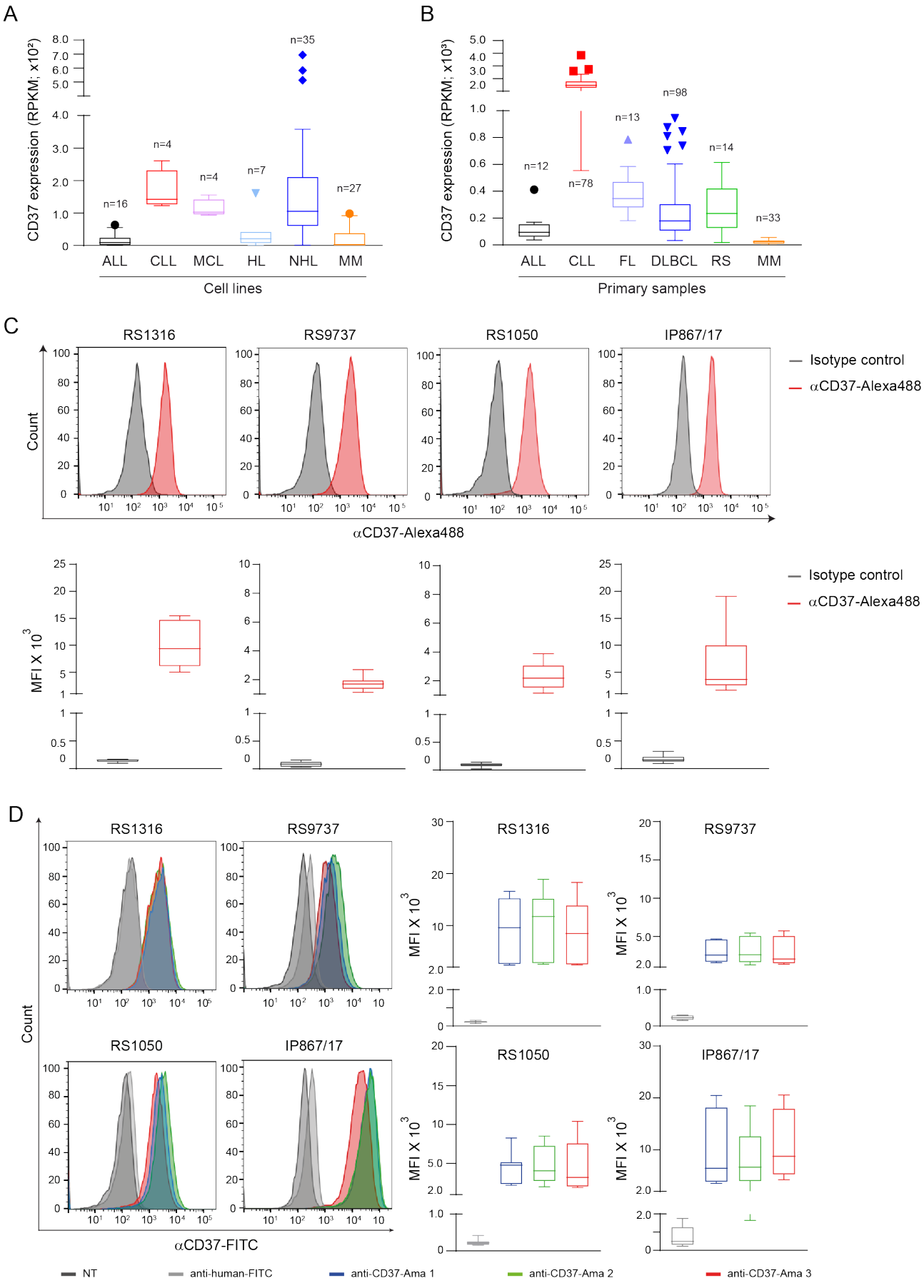
A
CD37 expression (RPKM; x10²)
n=16
n=4
n=4
n=7
n=35
n=27
ALL
CLL
MCL
HL
NHL
MM
Cell lines
B
CD37 expression (RPKM; x10³)
n=12
n=78
n=13
n=98
n=14
n=33
ALL
CLL
FL
DLBCL
RS
MM
Primary samples
C
RS1316
RS9737
RS1050
IP867/17
Count
αCD37-Alexa488
Isotype control
αCD37-Alexa488
MFI X 10³
Isotype control
αCD37-Alexa488
D
RS1316
RS9737
RS1050
IP867/17
Count
αCD37-FITC
MFI X 10³
NT
anti-human-FITC
anti-CD37-Ama 1
anti-CD37-Ama 2
anti-CD37-Ama 3

Figure S2

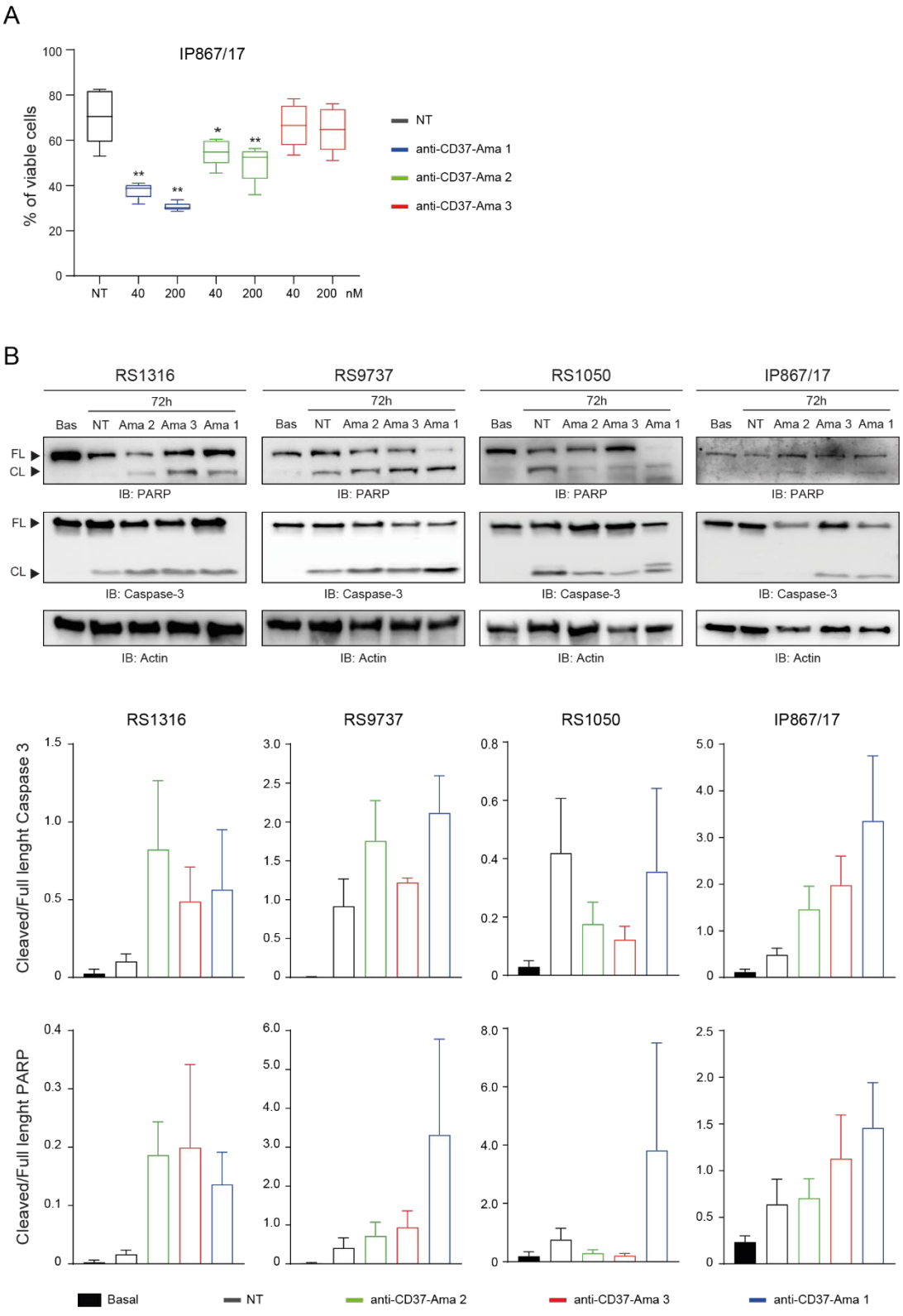
A
IP867/17
% of viable cells
NT
anti-CD37-Ama 1
anti-CD37-Ama 2
anti-CD37-Ama 3
NT 40 200 40 200 40 200 nM
B
RS1316
RS9737
RS1050
IP867/17
72h
Bas NT Ama 2 Ama 3 Ama 1
FL
CL
IB: PARP
IB: Caspase-3
IB: Actin
Cleaved/Full lenght Caspase 3
Cleaved/Full lenght PARP
Basal
NT
anti-CD37-Ama 2
anti-CD37-Ama 3
anti-CD37-Ama 1

Figure S3

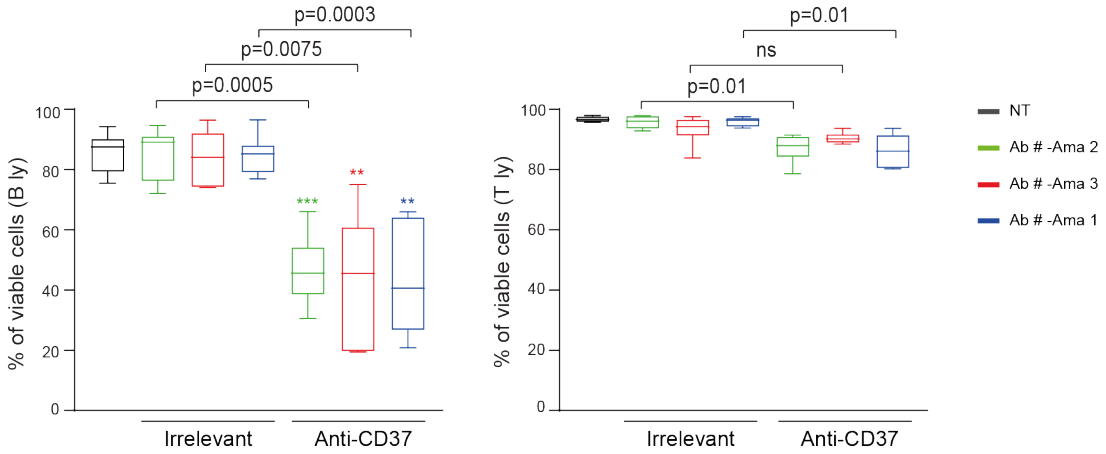
p=0.0003
p=0.0075
p=0.0005
% of viable cells (B ly)
100
80
60
40
20
0
***
**
**
Irrelevant
Anti-CD37
p=0.01
ns
p=0.01
% of viable cells (T ly)
100
80
60
40
20
0
Irrelevant
Anti-CD37
NT
Ab # -Ama 2
Ab # -Ama 3
Ab # -Ama 1

Figure S4

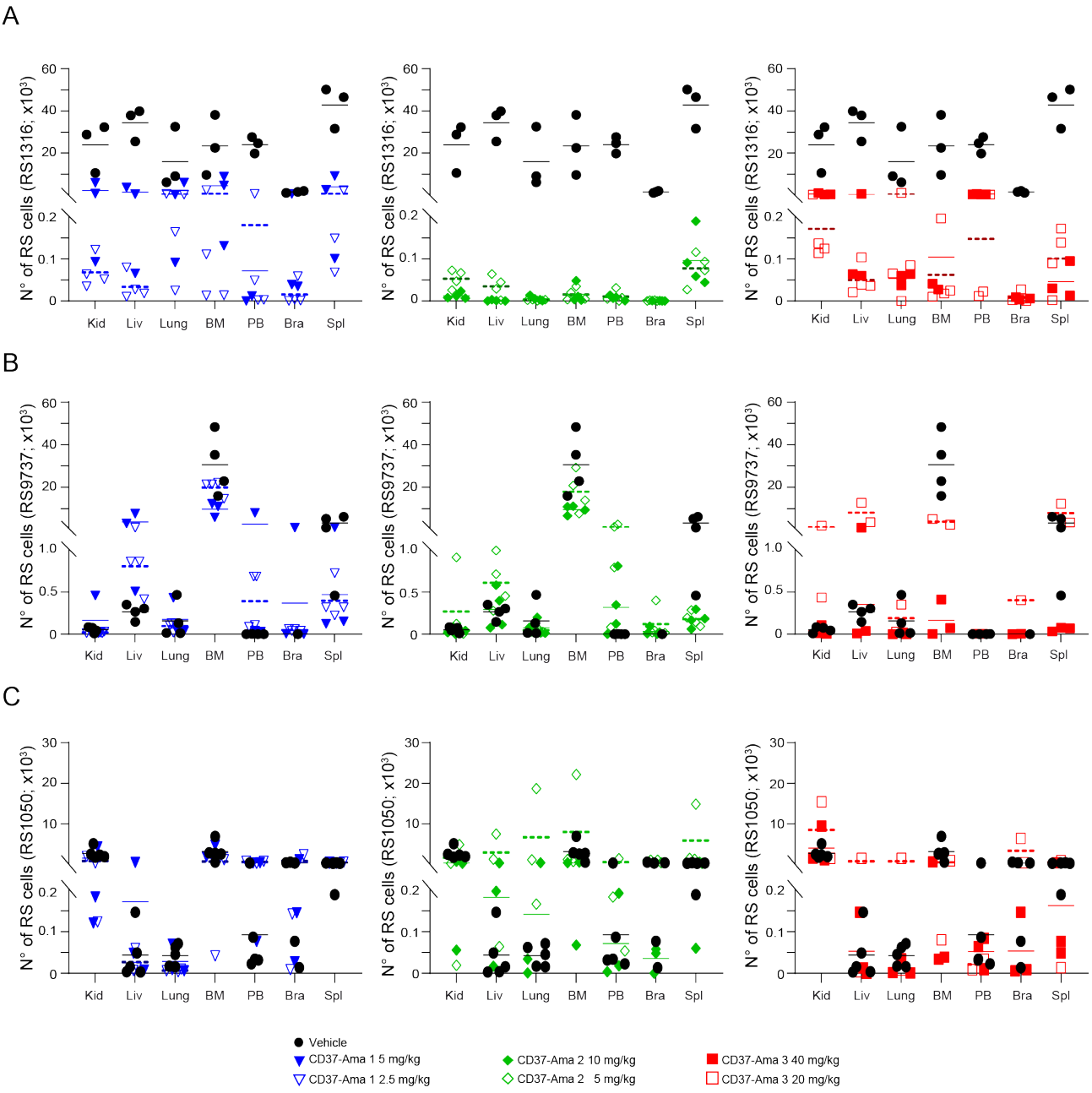
A
B
C
N° of RS cells (RS1316; x10³)
N° of RS cells (RS9737; x10³)
N° of RS cells (RS1050; x10³)
Kid
Liv
Lung
BM
PB
Bra
Spl
Vehicle
CD37-Ama 1 5 mg/kg
CD37-Ama 1 2.5 mg/kg
CD37-Ama 2 10 mg/kg
CD37-Ama 2 5 mg/kg
CD37-Ama 3 40 mg/kg
CD37-Ama 3 20 mg/kg

Figure S5

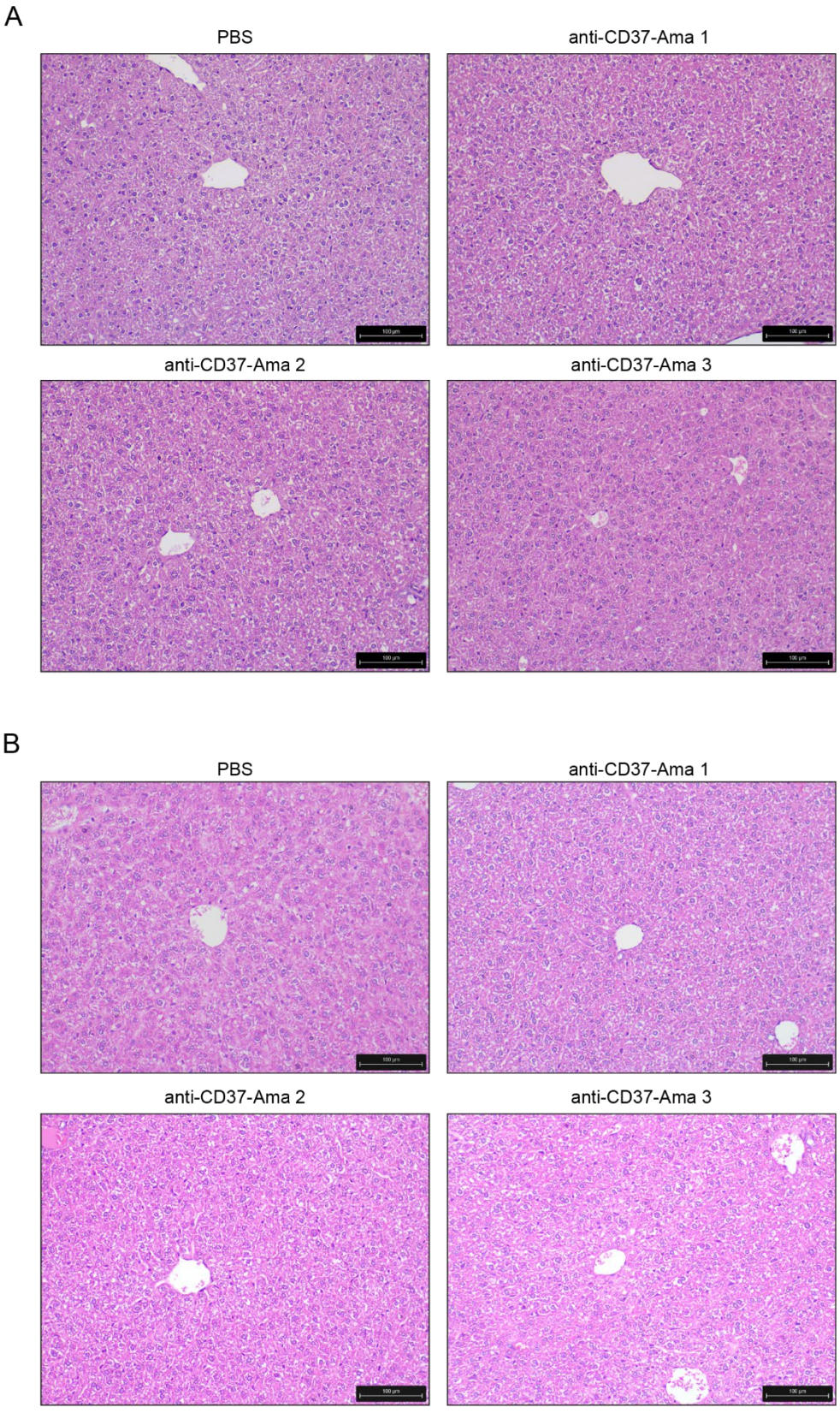
A
PBS
anti-CD37-Ama 1
anti-CD37-Ama 2
anti-CD37-Ama 3
B
PBS
anti-CD37-Ama 1
anti-CD37-Ama 2
anti-CD37-Ama 3

Figure S6